Available online at www.sciencedirect.com
ScienceDirect
Carbohydrate Research 343 (2008) 1346–1358
Carbohydrate RESEARCH

Structural characterization of the acid-degraded secondary cell wall polymer of *Geobacillus stearothermophilus* PV72/p2

Bent O. Petersen,[a] Margit Sára,[b,✠] Christoph Mader,[b] Harald F. Mayer,[b] Uwe B. Sleytr,[b] Martin Pabst,[c] Michael Puchberger,[c,†] Eberhard Krause,[d] Andreas Hofinger,[c] Jens Ø. Duus[a] and Paul Kosma[c,*]

[a]*Department of Chemistry, Carlsberg Laboratory, Gamle Carlsberg Vej 10, 2500 DK Valby, Denmark*
[b]*Center of Nanobiotechnology, University of Natural Resources and Applied Life Sciences, Gregor-Mendelstr. 33, A-1180 Vienna, Austria*
[c]*Department of Chemistry, University of Natural Resources and Applied Life Sciences, Muthgasse 18, A-1190 Vienna, Austria*
[d]*Leibniz-Institute of Molecular Pharmacology, Robert-Rössle-Str. 10, D-13125 Berlin, Germany*

Received 22 January 2008; received in revised form 18 March 2008; accepted 20 March 2008
Available online 30 March 2008

Abstract—The secondary cell wall polymer (SCWP) from *Geobacillus stearothermophilus* PV72/p2, which is involved in the anchoring of the surface-layer protein to the bacterial cell wall layer, is composed of 2-amino-2-deoxy- and 2-acetamido-2-deoxy-D-glucose, 2-acetamido-2-deoxy-D-mannose, and 2-acetamido-2-deoxy-D-mannuronic acid. The primary structure of the acid-degraded polysaccharide—liberated by HF-treatment from the cell wall—was determined by high-field NMR spectroscopy and mass spectrometry using N-acetylated and hydrolyzed polysaccharide derivatives as well as Smith-degradation. The polysaccharide was shown to consist of a tetrasaccharide repeating unit containing a pyruvic acid acetal at a side-chain 2-acetamido-2-deoxy-α-D-mannopyranosyl residue. Substoichiometric substitutions of the repeating unit were observed concerning the degree of N-acetylation of glucosamine residues and the presence of side-chain linked 2-acetamido-2-deoxy-β-D-glucopyranosyl units:

(**C**) (**D**) (**B**)
[-4)-β-D-Man*p*NAcA-(1-3)-β-D-Glc*p*N(Ac)$_{\sim 0.3}$-(1-6)-α-D-Glc*p*NAc-(1-]
3 4
| |
1 1
(β-D-Glc*p*NAc)$_{\sim 0.3}$ (**E**) (*S*)-Pyr-4,6-α-D-Man*p*NAc (**A**)

Keywords: *Geobacillus*; Secondary cell wall polymer; NMR spectroscopy; Mass spectrometry; Polysaccharide structure

1. Introduction

Crystalline bacterial cell surface layer (S-layer) proteins represent the outermost cell envelope component of many bacteria and archaea.[1–3] S-layers completely cover the cell surface during all stages of growth and division and they either exhibit oblique, square, or hexagonal lattice symmetry. Most S-layers are composed of single protein or glycoprotein species with molecular masses ranging from 40 to 200 kDa. The S-layer subunits are linked to each other by non-covalent forces. S-Layer proteins from gram-positive bacteria are bound to the rigid, peptidoglycan-containing layer via the so-called secondary cell wall polymers (SCWPs).[4–20] S-Layer proteins from *Bacillaceae* frequently carry an S-layer-homologous (SLH) domain on the N-terminal part.[21]

* Corresponding author. Tel.: +43 1 36006 6055; fax: +43 1 36006 6059; e-mail: paul.kosma@boku.ac.at
✠ Deceased May 2006.
† Present address: Institute of Material Sciences, TU Vienna, Getreidemarkt 9, A-1060 Vienna, Austria.

0008-6215/$ - see front matter © 2008 Elsevier Ltd. All rights reserved.
doi:10.1016/j.carres.2008.03.029

SLH-domains typically consist of three modules of about 55 amino acids from which 10 to 15 residues are conserved. Several studies indicated that SLH-domain carrying proteins bind to pyruvylated SCWPs.[5,9–11,14,16,17] Detailed studies regarding the interaction between an SLH-domain and the corresponding SCWP were carried out with the S-layer protein SbsB and the corresponding SCWP of *Geobacillus stearothermophilus* PV72/p2.[15] Surface plasmon resonance (SPR) spectroscopic measurements indicated the existence of three differently strong binding sites with low ($K_d = 2.6 \times 10^{-5}$ M), medium ($K_d = 6.1 \times 10^{-8}$ M), and high ($K_d = 6.7 \times 10^{-11}$ M) affinities. This feature was explained by heterogeneities always associated with naturally occurring heteropolysaccharides; although regarding the high affinity binding site, avidity effects resulting from the binding of SLH-domain dimers could not be completely excluded.[15] The recognition mechanism between the SLH-domain of SbsB and the SCWP of *G. stearothermophilus* PV72/p2 was found to be highly specific, as the SLH-domain neither recognized the peptidoglycan, nor pyruvylated SCWPs of other organisms. Furthermore, not the *N*-acetyl groups from the amino sugars but the pyruvic acid residues played a crucial role in the binding process.[15,17]

In previous studies, the structures of the acid-degraded and the native SCWP of *Bacillus sphaericus* CCM 2177 were elucidated by NMR spectroscopy analysis.[10,22] Contrary to the results obtained with the S-layer protein SbsB, the three SLH-motifs of the S-layer protein SbpA were not sufficient for binding to the corresponding SCWP of *B. sphaericus* CCM 2177, and a 58-amino acid long SLH-like motif located just behind the third SLH-motif was required for reconstituting the functional, SCWP-binding domain.[9]

In the present study, the structure of the HF-treated SCWP of *G. stearothermophilus* PV72/p2 was analyzed with the tools of NMR spectroscopy and mass spectrometry in combination with N-acetylation, Smith-degradation, and hydrolytic removal of pyruvic acid acetal residues.

2. Results and discussion

2.1. Chemical characterization and modification of the SCWP of *G. stearothermophilus* PV72/p2

Previous results on the linkage of SCWP to the peptidoglycan revealed the presence of pyrophosphate or phosphodiester bridges from 2-acetamido-2-deoxy-D-glucose to O-6 of muramic acid being susceptible to HF-induced cleavage.[28] Treatment of the SCWP of *G. stearothermophilus* PV72/p2 with HF at 4 °C afforded a polysaccharide material **1**, which was purified by GPC and eluted as a single peak. After hydrolysis of the GPC-purified

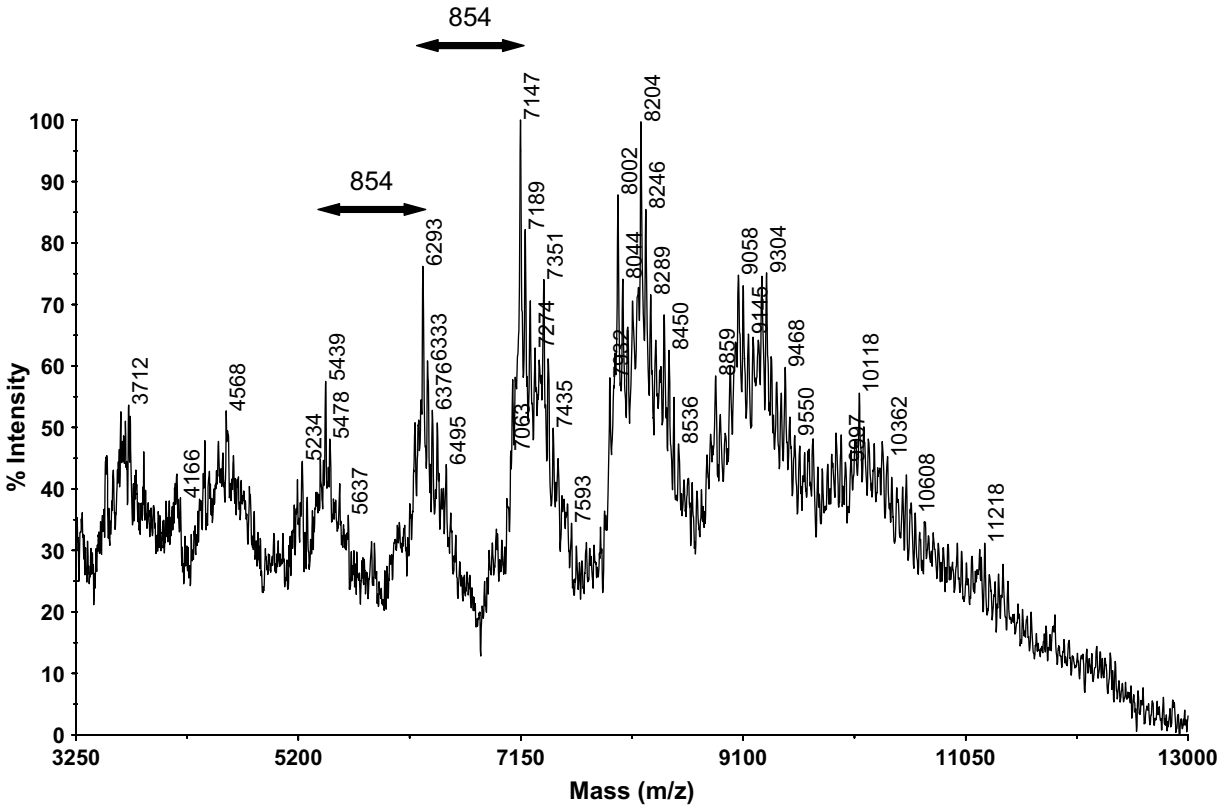

Figure 1. MALDI-TOF mass spectrum of the HF-treated secondary cell wall polymer **1** from *Geobacillus stearothermophilus* PV72/p2.

SCWP with 4 M HCl at 110 °C for 6 h, a molar ratio of 2-amino-2-deoxy-glucose to 2-amino-2-deoxy-mannose of ~2:1 was obtained.[23] In order to facilitate the structural analysis, a sequence of derivatization and degradation steps was performed comprising N-acetylation of polysaccharide **1**, which gave polysaccharide **2** followed by Smith-degradation and subsequent acid hydrolysis to afford polysaccharides **3** and **4**, respectively.

2.2. MALDI-TOF MS characterization of the SCWP of *G. stearothermophilus* PV72/p2

The MALDI mass spectrum of the HF-treated secondary cell wall polysaccharide **1** indicated substantial microheterogeneity of the sample with clusters of ions at *m*/*z* 5439, 6293, 7147, 8002 and multiple additional peaks separated by 42 Da mass difference. Furthermore, a second set of signals with reduced intensity was observed at *m*/*z* 6495, 7351, 8204, again displaying additional signals differing in 42 mass units (Fig. 1). The mass differences of 203–204 Da between the two signal clusters would indicate an additional acetamido-deoxy-hexose unit within the repeating unit, whereas the mass of 42 was indicative of the presence of additional acetyl groups. The observed mass differences of 854 between the major signals of the ion clusters would be consistent with the composition of a tetrasaccharide repeating unit $Pyr(HexNAc)_2HexNAcAHexN$.

2.3. NMR analysis of the HF-treated SCWP of *G. stearothermophilus* PV72/p2 (1) and chemically modified glycans (2–4)

For the interpretation of NMR data, capital bold letters refer to the individual monosaccharide residues as shown in Schemes 1 and 2 and Table 1. Primed bold letters designate substitution with hydrogen at the respective position. The structure analysis was based on one- and two-dimensional experiments obtained on a 800 MHz NMR spectrometer. In a first set of experiments, the major spectral features were used for a global characterization of the samples and to monitor the chemical modifications, followed by a detailed NMR analysis as outlined below.

The ^{1}H NMR spectrum of the HF-treated and GPC-purified polymer **1** displayed several clusters of signals in

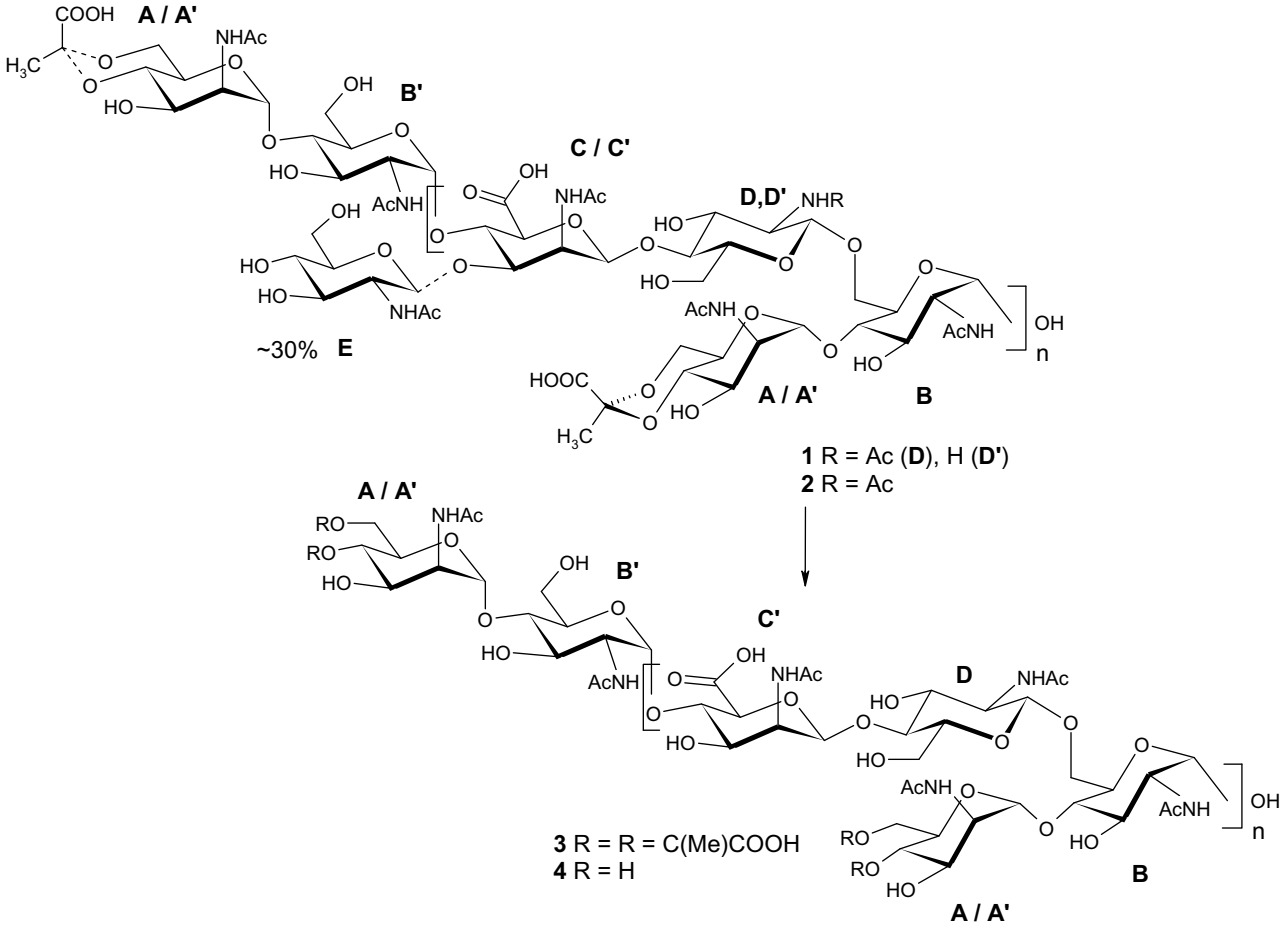

Scheme 1.

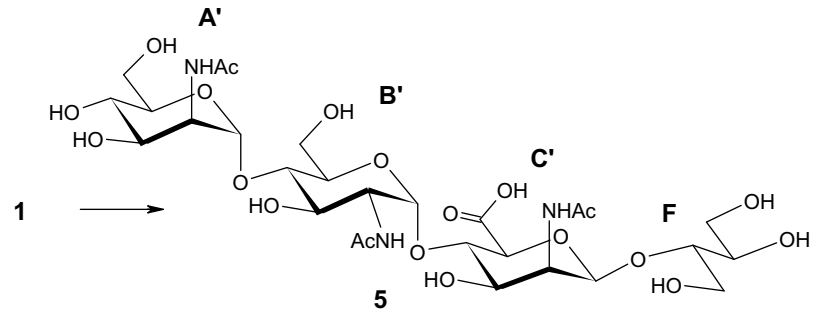

Scheme 2.

Table 1. NMR data of polysaccharides **1**–**4** and Smith-fragment **5**[a]

Atom H/C (ppm)		1	2	3	4	5	6a	6b	NHAc	CO	NOE/HMBC from H-1
Polysaccharide **1** *unit*											
α-PyrManNAc-1→	^{1}H	5.149	4.526	4.176	3.729	3.907	3.981	3.717	2.033		**B** 4
A	^{13}C	102.2	54.0	66.9	74.6	64.7	64.7		22.5	175.5	
Pyruvate	^{1}H	1.466									
	^{13}C	25.4									
→4,6-α-GlcNAc	^{1}H	5.233	3.885	3.88	3.634	3.88	4.084	3.891	2.033		**C** 4
B	^{13}C	98.1	54.1	71.1	78.9	70.5	69.7		22.5	175.5	**C′** 4
→3,4-β-ManNAcA	^{1}H	4.905	4.683	4.445	3.895	3.839			2.064		**D′** 4
C (30%)	^{13}C	99.8	49.1	75.2	71.2	77.5	175.6		22.7	175.2	
→4-β-ManNAcA	^{1}H	4.901	4.489	4.039	3.781	3.809			2.079		**D′** 4
C′ (70%)	^{13}C	99.9	54.2	73.3	74.4	77.6	175.6		22.6	176.1	
→4-β-GlcNH$_2$	^{1}H	4.771	3.149	3.844	3.789	3.552	3.923	3.794			**B** 6
D′	^{13}C	99.4	56.1	71.1	79.2	75.4	61.4				
β-GlcNAc-1→	^{1}H	4.555	3.586	3.540	3.302	3.467	3.985	3.666	2.005		**C** 3
E (25%)	^{13}C	96.3	56.3	74.3	71.4	74.8	61.9		22.7	174.8	
Polysaccharide **2** *unit*											
α-PyrManNAc-1→	^{1}H	4.814	4.571	4.193	3.709	3.852	3.971	3.727	2.032		**B** 4
A	^{13}C	103.5	54.3	67.0	74.9	64.7	65.1		22.7	175.3	
	$J_{C,H}$	178 Hz									
Pyruvate	^{1}H	1.466									
	^{13}C	25.5									
→4,6-α-GlcNAc	^{1}H	5.255	3.845	3.814	3.555	3.924	4.049	3.734	1.975		**C** 4
B	^{13}C	97.9	54.1	70.9	80.4	70.1	67.8		23.0	175.0	**C′** 4
	$J_{C,H}$	179 Hz									
→3,4-β-ManNAcA	^{1}H	4.904	4.690	4.453	3.899	3.811			n.d.[b]		**D** 4
C (30%)	^{13}C	100.1	49.2	75.2	71.4	77.7	n.d.				
	$J_{C,H}$	167 Hz									
→4-β-ManNAcA	^{1}H	4.906	4.477	4.016	3.782	3.805			2.069		**D** 4
C′ (70%)	^{13}C	100.0	54.3	73.4	74.6	77.7	n.d.		23.2	176.4	
→4-β-GlcNAc	^{1}H	4.418	3.692	3.724	3.698	3.479	3.883	3.723	n.d.		**B** 6
D	^{13}C	101.6	55.9	72.7	79.7	74.8	60.9		n.d.	n.d.	
	$J_{C,H}$	163 Hz									
β-GlcNAc-1→	^{1}H	4.583	3.585	3.563	3.307	3.472	3.986	3.668	n.d.		**C** 3
E	^{13}C	96.2	56.4	74.3	71.5	77.0	62.0				
	$J_{C,H}$	163 Hz									
Polysaccharide **3** *unit*											
α-PyrManNAc-1→	^{1}H	4.810	4.565	4.190	3.712	3.891	3.947	3.745	1.970		**B** 4
A	^{13}C	103.4	54.2	66.9	74.8	64.6	65.0		22.8	174.5	
Pyruvate	^{1}H	1.470									
	^{13}C	25.3									
→4,6-α-GlcNAc	^{1}H	5.252	3.848	3.808	3.558	3.910	4.041	3.730	2.030		**C′** 4
B	^{13}C	97.9	54.1	70.8	80.3	70.1	67.8		22.3	174.3	
→4-β-ManNAcA	^{1}H	4.908	4.476	4.017	3.794	3.803			2.080		**D** 4
C′	^{13}C	99.8	54.3	73.3	74.5	77.6	175.3		22.6	175.8	

(*continued on next page*)

Table 1 (*continued*)

Atom H/C (ppm)		1	2	3	4	5	6a	6b	NHAc	CO	NOE/HMBC from H-1
→4-β-GlcNAc	^{1}H	4.413	3.701	3.717	3.691	3.483	3.871	3.723	2.030		**B** 6
D	^{13}C	101.6	55.8	72.6	79.7	74.7	60.7		22.6	175.0	
Polysaccharide **4** *unit*											
α-ManNAc-1→	^{1}H	4.835	4.522	4.069	3.575	3.818	3.86	3.86	2.029		**B** 4
A′	^{13}C	102.7	53.8	69.9	67.5	73.8	61.3		22.5	175.2	
→4,6-α-GlcNAc	^{1}H	5.251	3.825	3.814	3.550	3.908	4.033	3.797	2.029		**C′** 4
B	^{13}C	97.9	54.2	70.9	80.4	70.2	68.0		22.6	175.0	
→4-β-ManNAcA	^{1}H	4.908	4.462	4.009	3.776	3.778			2.074		**D** 4
C′	^{13}C	99.8	54.4	73.5	74.4	77.8	175.6		22.7	176.0	
→4-β-GlcNAc	^{1}H	4.556	3.710	3.726	3.697	3.474	3.864	3.719	2.023		**B** 6
D	^{13}C	101.7	56.0	72.8	79.7	75.0	60.8		22.9	174.8	
Trisaccharide fragment **5** *unit*											
α-ManNAc-1→	^{1}H	5.228	4.468	4.040	3.613	3.768	3.86	3.86	2.03		**B′** 4
A′	*J* (Hz)	1.3	4.5	9.8	9.8	6.6	n.d.				
	^{13}C	101.0	53.4	69.6	67.1	73.8	60.8		22.5	175.2	
→4-α-GlcNAc	^{1}H	5.286	3.875	3.891	3.693	3.835	3.79	3.79	2.03		**C′** 4
B′	*J* (Hz)	2.4	10.9	n.d.	n.d.	6.1	12.0				
	^{13}C	97.7	54.3	71.6	76.6	71.1	60.6		22.5	175.0	
→4-β-ManNAcA	^{1}H	4.885	4.448	4.012	3.800	3.771			2.073		**F 2**
C′	*J* (Hz)	1.0	4.5	9.8	n.d.						H5/C′6
	^{13}C	99.7	54.5	73.4	74.2	77.7	176.0		22.7	176.1	
→2 erythritol	^{1}H	3.694	3.773	3.769	3.783						
		3.569			3.701						
F	^{13}C	62.7	82.0	73.8	61.3						

[a] Due to the heterogeneity of the samples and partial hydrolysis of pyruvate groups upon standing, a full assignment of units **A′** and **D** in polysaccharide **1** and unit **A′** in **2** could not be accomplished.
[b] n.d. Not determined.

the anomeric region between δ 5.48 and 4.50, other pyranose proton signals between δ 4.68 and 3.15, methyl group signals of acetamido moieties between δ 2.08 and 2.00, and a methyl singlet at 1.47 ppm (Fig. 2). The latter signal was identified as the methyl group of a pyruvic acid acetal by the observed HMBC-connectivity of the CH_3 protons to ^{13}C NMR signals at ~102 (C-2) and at ~176 ppm (C=O). Major anomeric signals derived from the repeating units of the polysaccharide clustered into two groups of approx. 3:1 intensity ratio. All anomeric protons could be correlated via H2BC and HMBC experiments to C-2 carbon signals with chemical shift values characteristic of nitrogen-bearing carbons, thereby proving 2-amino-2-deoxysugars as the only monosaccharide constituents of the polymer. Since in the ^{13}C NMR spectrum signals from non-anomeric carbohydrate carbons in the region δ 82–88 were not observed, all monosaccharide constituents were in the pyranose form. The assignments of the anomeric configuration of the monosaccharides were based on the values of the hetero-nuclear $J_{C\text{-}1,H\text{-}1}$ coupling constants of the anomeric carbons measured in the N-acetylated polysaccharide **2**. Thus, the α-anomeric configuration was established for residues **A** and **B** ($J_{C\text{-}1,H\text{-}1}$ 178 and 179 Hz, respectively), and the β-anomeric configuration was found for residues **C**, **D**, and **E** ($J_{C\text{-}1,H\text{-}1}$ 163 and 167 Hz, Table 1).[29] The ^{1}H NMR spectra of the N-acetylated polysaccharide **2** and the Smith-degraded polysaccharide **3** showed an increase of signal intensities of the *N*-acetyl signals in relation to the pyruvic acid methyl groups. The observed ratio of ~4:1 in polysaccharide **3** suggested the presence of four acetamidodeoxysugars and near stoichiometric substitution of one residue by a pyruvic acetal in the repeating unit. Smith-degradation of polysaccharide **2** furnished polysaccharide **3** and led to the removal of a set of NMR signals, assigned to residue (**E**), which were present in about 30% of polysaccharides **1** and **2** (Fig. 2). Subsequent hydrolysis of the Smith-degraded polysaccharide **3** with acetic acid at 110 °C resulted in the cleavage of the pyruvic acid acetals and gave polysaccharide **4** (Scheme 1).

2.3.1. NMR analysis of the Smith-degraded N-acetylated polysaccharides 3 and 4. The 800 MHz ^{1}H NMR spectrum of the Smith-degraded, N-acetylated polysaccharide **3** showed four major anomeric signals being consistent with the presence of a tetrasaccharide repeating unit. In addition, a minor set of anomeric protons was observed indicating the presence of chain-terminating distal end groups and of reducing end units (Fig. 2). For unit **A**, small homo-nuclear coupling constants $J_{H,H}$ were observed for the signal of H-2 (δ 4.565) at a low-field. In conjunction with the coupling constants of the

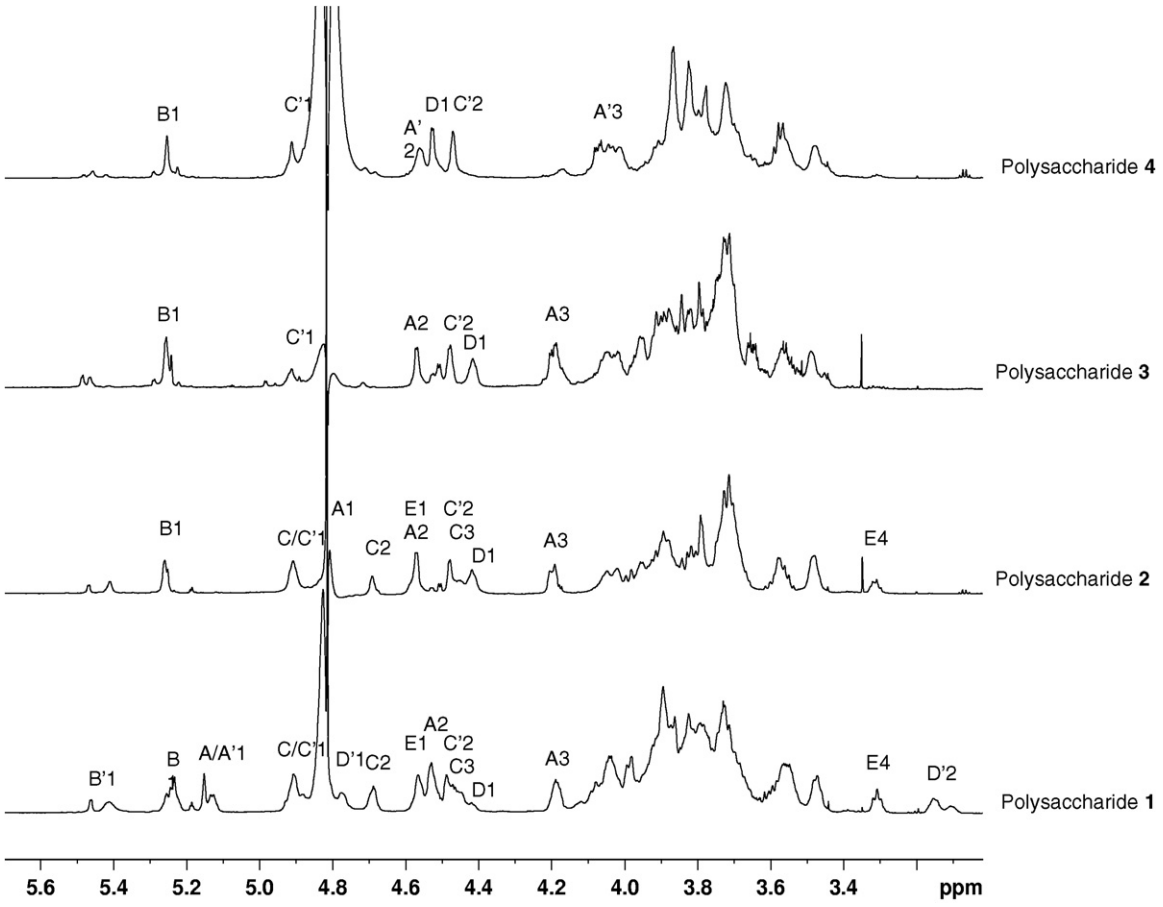

Figure 2. Stacked plots of the 800 MHz ^{1}H NMR spectra displaying the anomeric and bulk region of polysaccharides **1**–**4**. Arabic numerals refer to the respective protons in sugar units as labeled in Scheme 1.

correlated H-3 signal at 4.190 ppm ($J_{2,3} \sim 4.5$, $J_{3,4} \sim 9.5$ Hz) and the corresponding ^{13}C NMR shift data, residue **A** was identified as a 2-acetamido-2-deoxy-α-mannopyranose unit. A complete assignment of the proton and carbon connectivities within the 2-acetamido-2-deoxy-α-mannopyranosyl unit **A** and the other monosaccharide units **B**, **C**′, and **D** was achieved using the edited HSQC/H2BC experiments (Fig. 3). The H2BC technique almost exclusively correlates protons and proton-bearing carbon spins separated by two covalent bonds and is independent of occasionally vanishing $^{2}J_{CH}$ coupling constants and thereby allows to distinguish two- and three-bond correlations in HSQC-TOCSY or HMBC spectra (Fig. 3).[24] The ^{1}H and ^{13}C NMR chemical shifts derived from ^{1}H, ^{1}H-COSY, and ^{1}H, ^{13}C-HSQC correlation measurements were then used to identify residue **B** as a 2-acetamido-2-deoxy-α-glucopyranosyl unit and residue **D** as a 2-acetamido-2-deoxy-β-glucopyranosyl unit. The presence of a *manno*-configured 2-acetamido-2-deoxy-pyranosyluronic acid residue **C**′, which had not been detected by the previous chemical characterization,[23] was established via HSQC and HMBC correlation experiments. These experiments allowed to follow the connectivities of the N-linked carbons to the carbonyl signals of the 2-acetamido groups of the units **A**, **B**, **C**′, and **D** in polysaccharide **4**, respectively, with additional correlations being observed from C-4 and C-5 of unit **C**′ to a carbonyl signal at position 6 (δ 175.3).

Analysis of the ^{13}C NMR low-field chemical shifts of residues **A**–**D** in polysaccharide **3** suggested the substitution of C-4 (δ 74.8) and C-6 (δ 65.0) of the 2-acetamido-2-deoxy-α-mannopyranosyl unit **A**, C-4 (δ 80.3) and C-6 (δ 67.8) of the 2-acetamido-2-deoxy-α-glucopyranosyl unit **B**, C-4 for 2-acetamido-2-deoxy-β-mannuronic acid **C**′ (δ 74.5), and C-4 for the 2-acetamido-2-deoxy-β-glucopyranosyl unit **D** (δ 79.7), respectively (Table 1). A nuclear Overhauser effect interaction was observed from the anomeric proton of residue **A** to H-4 of unit **B**. Since NOE-interactions from the other sugar units as well as ^{13}C NMR glycosylation shifts other than those at C-4 and C-6 in unit **A** were absent, 2-acetamido-2-deoxy-α-mannopyranosyl unit **A** was assigned as a side chain unit being substituted by a pyruvic acid acetal at *O*-4 and *O*-6. NOE-interactions and HMBC correlations were then used to establish the sequence of sugars in the main chain. Thus, H-1 of unit **B** gave an NOE to H-4 of **C**′, while H-1 of unit **C**′ was correlated to H-4 of unit **D**,

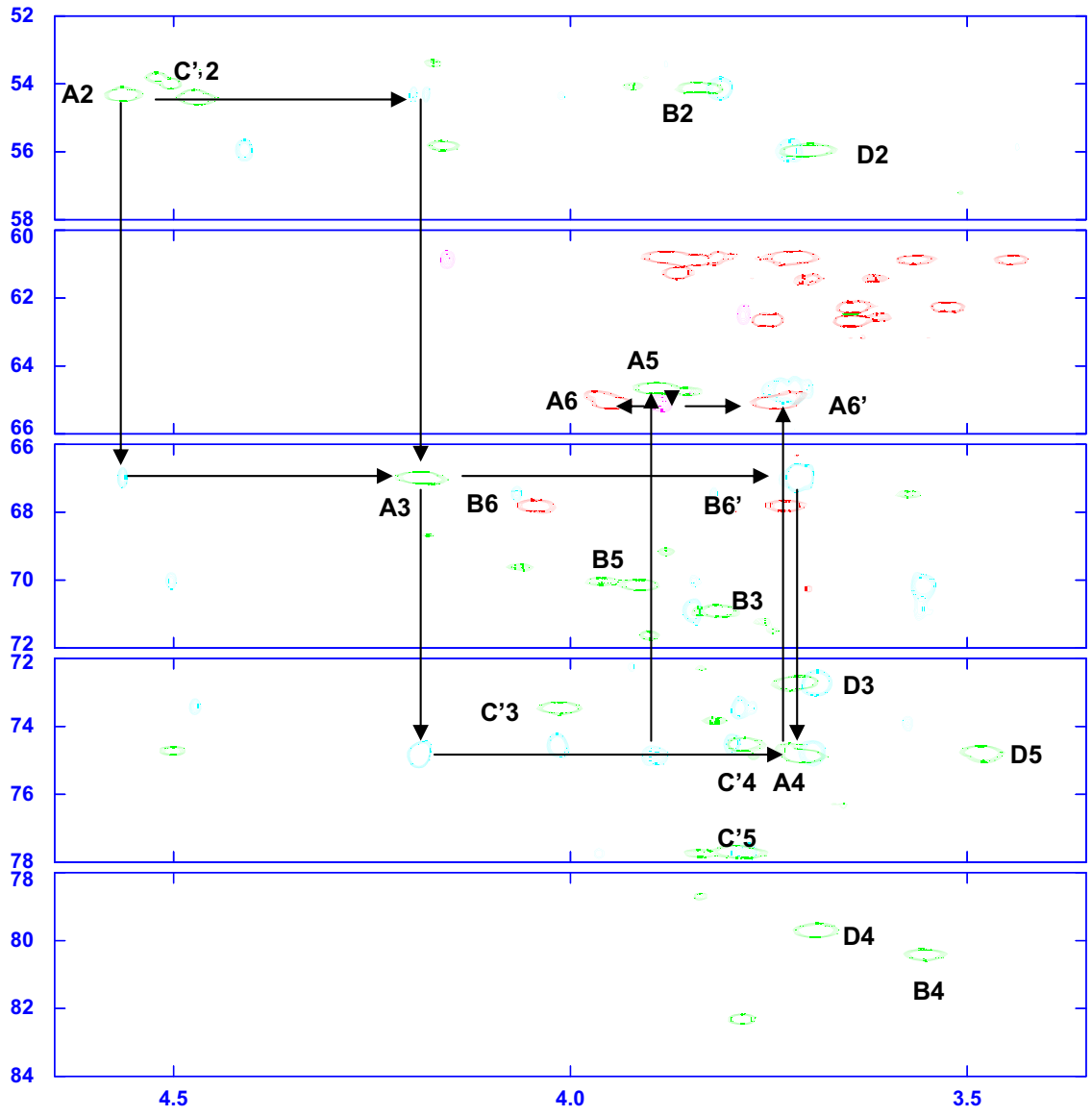

Figure 3. The figure shows an edited HSQC (green/red) and an edited H2BC (cyan/magenta) plot of the bulk region of polysaccharide **3** to follow through the spinsystem of the 4,6-pyruvate-α-ManNAc unit **A**. Starting from C2 (green) gives connectivity to C3 via a three-bond correlation in H2BC (cyan). Further connectivity is established through C4 to C5 and via a H2BC (magenta) to the CH_2 of C6 (red).

and H-1 of residue **D** gave NOE's to the geminal H-6 protons of the 2-acetamido-2-deoxy-α-glucopyranosyl unit **B**. Hence, the sequence **B**→**C**′→**D** was established, wherein unit **B** is substituted at O-4 with the pyruvate-containing 2-acetamido-2-deoxy-α-mannopyranosyl unit **A**. The assignment of the *S*-configuration of the pyruvic acid acetal was based on the chemical shift of the ^{13}C NMR signal of C-2 at 25.1 ppm.[25,26]

Eventually, the pyruvic acid substituents were removed by acid degradation of the polysaccharide preparation **3** with 1% acetic acid at 110 °C to furnish the polysaccharide derivative **4**. Whereas the ^{13}C NMR signals for units **B** and **C**′ in sample **4** remained nearly unchanged, C-4 and C-6 of the 2-acetamido-2-deoxy-α-mannopyranosyl unit **A**′ were now observed at high-field, confirming that residue **A** in polysaccharide **3** contains the pyruvic acid acetal substituent (Table 1).

2.3.2. Analysis of an oligosaccharide fragment derived from Smith-degradation of the HF-treated SCWP 1. Smith-degradation of the SCWP-derived polysaccharide **1** led to significant hydrolysis of the polysaccharide backbone and loss of side chain residues. The resulting oligosaccharide fragments were separated by GPC into several pools containing tri- up to octasaccharide fragments (data not shown). Within these low molecular weight fractions, one pool contained a trisaccharide fragment **5** mixed with a smaller fraction of a tetrasaccharide fragment (Scheme 2).

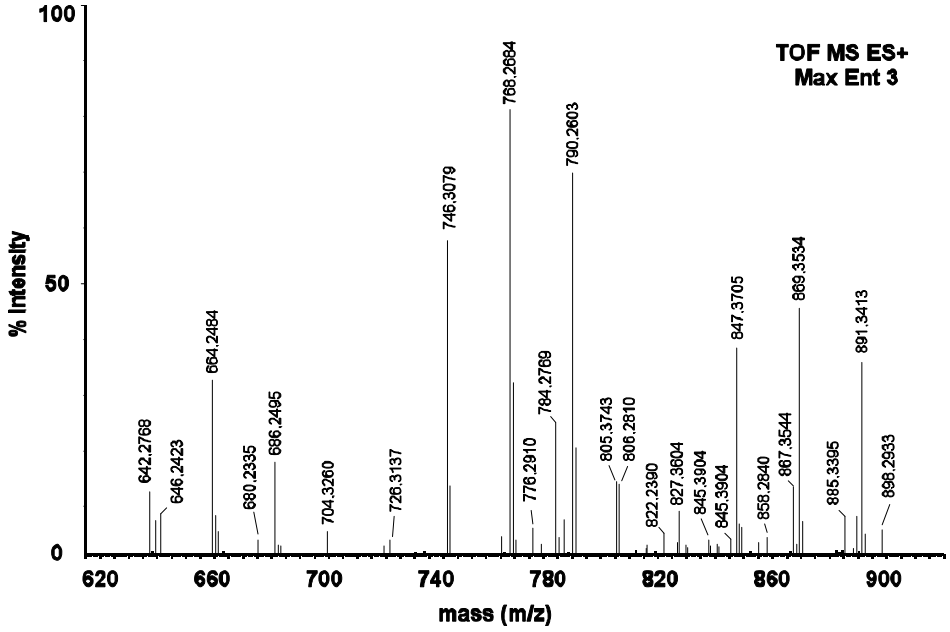

Figure 4. ESI-TOF mass spectrum (positive mode) of the trisaccharide fragment **5** obtained by Smith- degradation.

ESI-TOFMS data of the mixture recorded in the positive ion mode furnished a molecular ion at *m*/*z* 746.3151 in addition to mono- and disodium adducts (Fig. 4). The composition of the major ion was consistent with the presence of $(HexNAc)_2$-HexNAcA-tetritol. In addition, a tetrasaccharide species was observed at *m*/*z* 847.3705. Further fragmentation of the tetrasaccharide molecular ion indicated the loss of one HexNAc residue from the reducing end with further fragmentation patterns containing the HexNAcA moieties (data not shown). These data would thus indicate a sequence of HexNAc-HexNAc-HexNAcA-HexNAc units (Fig. 5).

The NMR data of **5** could be fully assigned and confirmed the structural assignment of the carbohydrate residues. The ^{1}H NMR spectrum revealed two signals of anomeric protons at low-field (δ 5.228 for unit **A**′ and δ 5.286 for **B**′) and one anomeric proton shifted to higher field (δ 4.885 for residue **C**′). All anomeric signals exhibited small values for the $J_{1,2}$ coupling constants in a range of 1–2.4 Hz. The values of the coupling constants of the pyranose ring protons confirmed the presence of *manno*-configured sugars **A**′ and **C**′ and 2-acetamido-2-deoxy-α-glucopyranose for unit **B**′ (Table 1). The identity of unit **C**′ as 2-acetamido-2-deoxy-α-mannopyranosyluronic acid was confirmed on the basis of the observed HMBC-correlation of H-5 to a downfield-shifted carbonyl signal at δ 176.0 (Fig. 4). The inter-unit linkages and the sequence were derived from the high-field-shifted carbon signals of C-4 for **B**′ (δ 76.6) and **C**′ (δ 74.2), the HMBC-correlations from H-1 of the terminal α-ManNAc residue **A**′ to C-4 of unit **B**′ and from H-1 of residue **B**′ to C-4 of residue **C**′. Finally, H-1 of unit **C**′ displayed HMBC-connectivity and NOESY interactions to position 2 (δ 82.0) of D-*erythritol*, arising from a Smith-degraded 4-O-substituted 2-amino-2-deoxy-glucose moiety.[27]

2.3.3. NMR analysis and the structure of the HF-treated secondary cell wall polymer 1 and its N-acetylated derivative 2. On the basis of the structural assignments of polysaccharides **3** and **4** as well as the trisaccharide fragment **5**, the spectra of the HF-treated SCWP **1** and its N-acetylated derivative **2** could be assigned. In the 800 MHz ^{1}H NMR spectra of the latter two polysaccharides additional signals were seen in the anomeric region and at the high-field end of the bulk region (Fig. 2). The high-field signal at δ 3.15 of the SCWP polysaccharide **1** was identified as H-2 of a 2-amino-2-deoxy-β-glucopyranosyl unit (**D**′), being correlated to H-1 ($J \sim 8$ Hz) at δ 4.77. Following the N-acetylation step, this anomeric proton was not observed any more, but led to increased signal intensity for the anomeric signal of unit **D** at δ 4.42.

In addition, N-acetylation resulted in the shift of the apparent triplet ($J \sim 9$ Hz) in the high-field region at δ 3.15 into the bulk region of the pyranose ring protons (Fig. 2). The second triplet signal at high-field (δ 3.30) could be assigned to H-4 of the 2-acetamido-2-deoxy-β-D-glucopyranosyl unit **E**. The signal intensity of residue **E** corresponded to ~30% relative to those of the tetrasaccharide repeating unit in polysaccharides **1** and **2**. Since glycosylation shifts were absent in the ^{13}C NMR data of this residue, unit **E** corresponds to a side chain residue being susceptible to periodate oxidation (Table 1). The linkage site of unit **E** to the polysaccharide chain was finally assigned on the basis of the

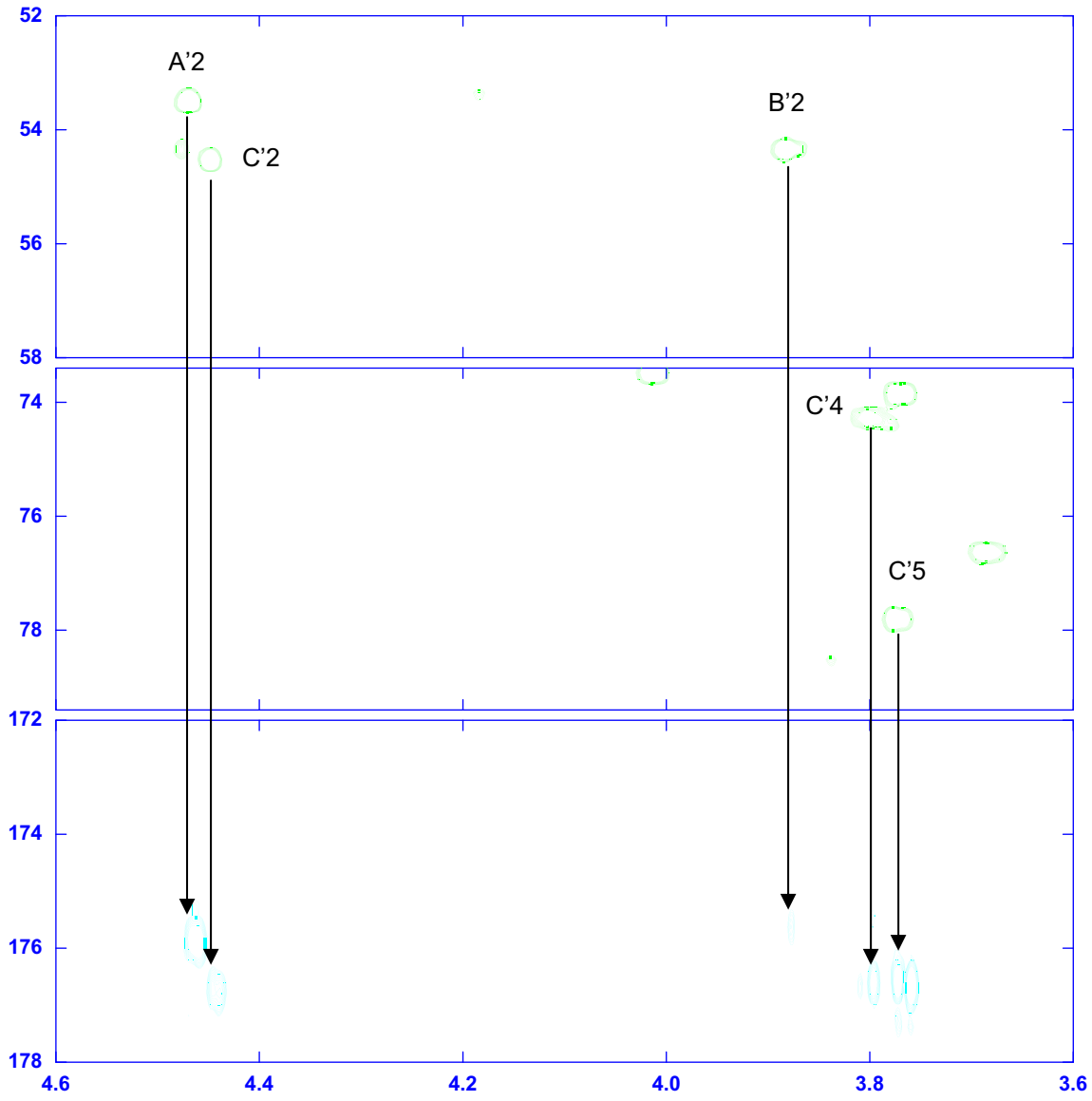

Figure 5. HSQC (green) and HMBC (cyan) plot of oligosaccharide **5** providing the correlations of C2 in α-ManNAc (**A**′), β-ManNAcA (**C**′), and α-GlcNAc (**B**′) to the respective carbonyl signals and the correlation from β-ManNAcA (**C**′) C4 and C5 to the carbonyl C6 signal.

observed NOE from H-1 of unit **E** to H-3 of unit **C**. Further support was derived from the low-field shifted ^{13}C NMR signal of carbon 3 of unit **C** accompanied by a high-field shift of the neighboring C-2 and C-4 carbon signals (Table 1).

Additional minor signals in the anomeric region indicated the presence of reducing end groups of 2-acetamido-2-deoxy-glucopyranosyl units, of chain-terminating end groups of the polysaccharide, and of unsubstituted 2-acetamido-2-deoxy-α-mannopyranosyl units **A**′. The formation of reducing ends assigned to 2-acetamido-2-deoxy-glucopyranosyl moieties with anomeric $^{1}H/^{13}C$ NMR shifts at δ 5.20/ 91.2 and δ 4.69/95.5, respectively, indicates that this sugar provides the linkage to the peptidoglycan (Fig. 6). Upon standing, partial hydrolysis of the carboxyethylidene groups led to even more complex spectra as reflected in the HSQC-spectrum of **1** (Fig. 6). The anomeric signals of polysaccharide **1** were strongly influenced by the degree of pyruvate substitution at the 2-acetamido-2-deoxy-mannose units **A** and depending on whether the internal unit **D** occurred with a free amino group or the *N*-acetamido substituent at C-2 (Fig. 6). Notably, N-acetylation of the amino group of residue **D** had a pronounced effect on the anomeric proton and carbon signals of the neighboring 2-acetamido-2-deoxy-mannose unit **A**.

In conclusion, the combined evidence of the NMR and mass spectral characteristics is consistent with the proposed structure for the repeating unit of the acid-degraded secondary cell wall polymer as

(C) (D) (B)
[-4)-β-D-Man*p*NAcA-(1-3)-β-D-Glc*p*N(Ac)$_{\sim 0.3}$-(1-6)-α-D-Glc*p*NAc-(1-]
3 4
| |
1 1
(β-D-Glc*p*NAc)$_{\sim 0.3}$ (**E**) (*S*)-Pyr-4,6-α-D-Man*p*NAc (**A**)

Recently, the structures of other secondary cell wall polymers have been reviewed and placed into three different groups.[28] Group I comprises a backbone of alternating β-(1→3)- and β-(1→4)-linkages between 2-acetamido-2-deoxy-mannose and 2-acetamido-2-deoxy-glucose residues. The disaccharide repeating unit may additionally contain 4,6-linked pyruvic acid substituents at the 2-acetamido-2-deoxy-mannose moieties as shown for *Paenibacillus alvei* CCM 2051 and *Bacillus sphaericus* CCM 2177 or may contain substoichiometric amounts of α-ribofuranosyl side-chain units.[30] Other *Geobacillus* strains harboring tetrasaccharide repeats with 2,3-diacetamido-2,3-dideoxy-mannuronic acid, glucose, and 2-acetamido-2-deoxy-glucose as sugar constituents were compiled in group II.[30] One example of an SCWP isolated from *Aneurinibacillus thermoaerophilus* DSM 10155 was reported with an unusual biantennary structure being composed of 2-acetamido-2-deoxy-mannose, 2-acetamido-2-deoxy-glucose, and 2-acetamido-2-deoxy-galactose and has been placed into group III.[31] The linkage of secondary cell wall polymers to the peptidoglycan matrix has been investigated using intact SCWP–peptidoglycan complexes and provided evidence that these polysaccharides are linked to the 6-position of *N*-acetylmuramic acid via phosphodiester or pyrophosphate bridges.[22,30–32] The structure of the SCWP from *G. stearothermophilus* PV72/p2 loosely resembles group II polysaccharides by the presence of a flexible 6-*O*-glycosyl linkage, which is also present in a major cell wall polysaccharide of *Bacillus anthracis*.[33] Unique features, however, pertain to the presence of basic 2-amino-2-deoxy-glucopyranose units in the chain leading to a zwitterionic character of the polymer and to the presence of two different side chain residues. Approx. 30% of 2-acetamido-2-deoxy-β-mannopyranose units were substituted at O-3 with 2-acetamido-2-

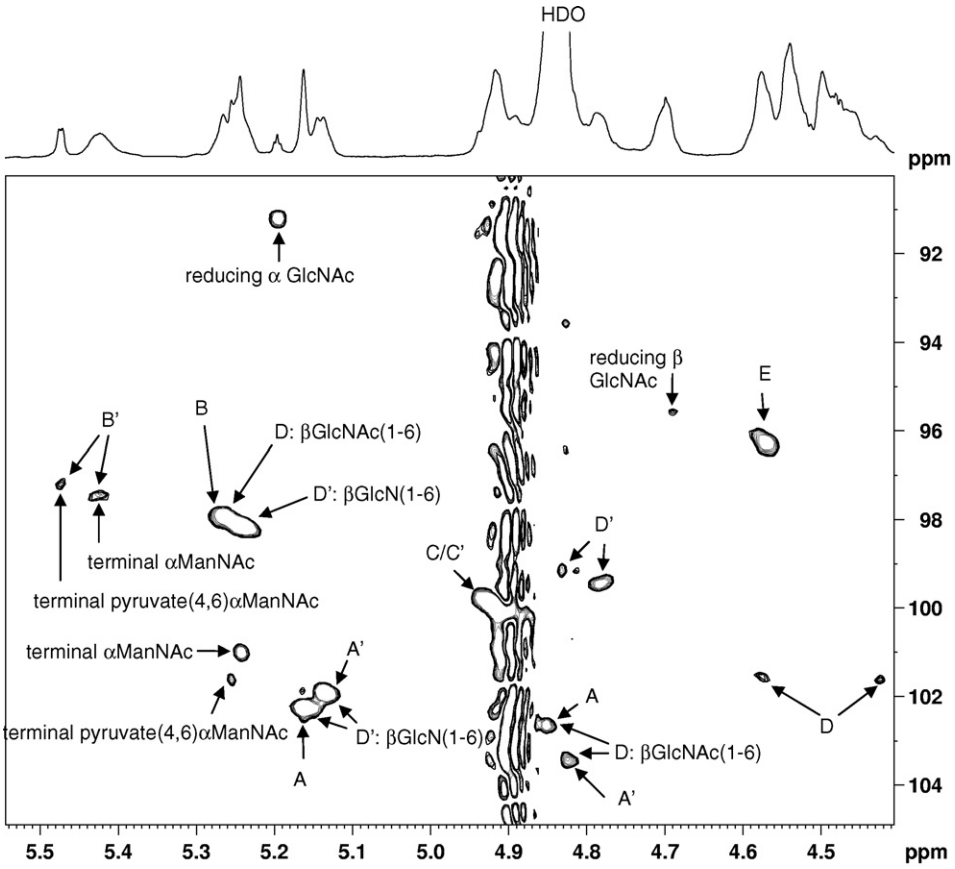

Figure 6. HSQC-spectrum of the anomeric region of the acid-degraded secondary cell wall polymer **1**. The spectrum shows the diversity of the polymer including reducing end, chain-terminating end groups (indicated as terminal ManNAc groups), and local effect on the shifts due to heterogeneity. All shifts are assigned, but only the main shifts are included in Table 1.

deoxy-β-glucopyranose residues, which were subsequently completely removed by Smith-degradation. The second side chain moiety was found to be an α-linked 2-acetamido-2-deoxy-mannopyranose residue, which was almost completely substituted by pyruvic acid acetal groups, thereby most likely providing the anchoring function of the polymer. Since the polysaccharide had been isolated by HF-treatment, loss of pyruvic acid residue or partial hydrolysis of glycosyl residues of the native material, however, cannot be excluded and a complete structural elucidation of the secondary cell wall polymer will have to rely on the isolation of the intact material including the peptidoglycan linkage region. The microheterogeneity of the acid-degraded polysaccharide hampered a straightforward structural elucidation of the polymer and hence defined modification and degradation steps were necessary. Thus, in order to facilitate spectral assignments, the polysaccharide was subjected to N-acetylation, followed by Smith-degradation and hydrolytic removal of the pyruvate residues to give a polysaccharide material containing a homogeneous tetrasaccharide repeating unit. Smith-degradation of the polysaccharide, which still contained the free amino groups at the internal 2-amino-2-deoxy-β-glucopyranose, led to the substantial hydrolysis of the polysaccharide backbone accompanied by the removal of the side chain 2-acetamido-2-deoxy-β-glucopyranose moieties. Eventually, a trisaccharide fragment could be isolated and structurally analyzed from the Smith-degraded material, which most likely originated from adjacent tetrasaccharide repeating units containing two sequential internal 2-amino-2-deoxy-β-glucopyranose units **D′** without *N*-acetyl substituents. The molecular weight of the SCWP was estimated from the MALDI-TOF data to correspond to 7–10 repeating units, which is in fair agreement with surface plasmon resonance data indicating an approximate value of 10 kDa.[15]

3. Experimental

3.1. Growth of *G. stearothermophilus* PV72/p2 and preparation of cell wall fragments

G. stearothermophilus PV72/p2 was grown on SVIII-medium with glucose as carbon source under oxygen-limited conditions at 57 °C in continuous culture at a dilution rate of 0.1 h^{-1}.[7,18] Cell wall fragments were prepared as described in a previous study.[18] For extracting the S-layer protein and other cell wall-associated protein, cell wall fragments were treated with 1% aq sodium dodecyl sulfate (SDS) at 100 °C for 30 min. After centrifugation of the suspension at 40,000*g* at 20 °C for 20 min, the pellet was washed at least five times with water (A. purif. HPLC-grade).

3.2. Extraction of the SCWP

For extracting the SCWP, 500 mg of lyophilized, SDS-treated cell wall fragments were incubated in 10 mL of 48% hydrofluoric acid (HF) at 0 °C for 48 h in a well-ventilated hood using Teflon-material. After centrifugation of the suspension at 40,000*g* at 4 °C for 30 min, the clear supernatant was carefully removed. SCWP was precipitated by adding the fivefold volume of chilled dry ethanol (−20 °C) and incubating the suspension at −20 °C for 20 h. Subsequently, the suspension was centrifuged at 20,000*g* at −10 °C for 20 min, and the pellet washed twice with chilled ethanol (−20 °C). After dissolving in distilled water, the samples were frozen at −20 °C and the HF-extracted SCWP was lyophilized.

3.3. Purification of the SCWP by gel permeation chromatography (GPC)

For purification by GPC, lyophilized SCWP (10 mg) was dissolved in a soln of 5 mM aq ammonium acetate (800 μL) and applied to a Superdex 75 HiLoad™ 16/60 column (Pharmacia) using 5 mM ammonium acetate for elution. Fractions containing SCWP were detected with a refraction index (RI) detector (Knauer), pooled and dialyzed against A. purif. HPLC-grade at 4 °C for 18 h. Then, the pH value was adjusted to 7.2 with 0.1% aq NH_3, the soln was frozen at −20 °C, and lyophilized to give **1**. Chemical analysis was performed as described in a previous study.[23]

3.4. N-Acetylation of GPC-purified SCWP

For N-acetylation of amino sugars, 50 mg GPC-purified SCWP was dissolved in 0.8 M aq $NaHCO_3$ (20 mL) and the sample was cooled down to 4 °C. Ten portions of Ac_2O (each 100 μL) were added in 20 min intervals and the pH value was kept constant at 8.2 by the addition of 1 M NaOH. After a total reaction time of 5 h, the soln was dialyzed against water at 20 °C for 18 h. Subsequently, the pH value was adjusted to 7.2 as described above and the samples were lyophilized to give polysaccharide **2**.

3.5. Smith-degradation and acid hydrolysis

About 20 mg of **2** was dissolved in 30 mM sodium acetate buffer (20 mL, pH 5.3), which contained 20 mM sodium periodate and the soln was incubated in the dark at 4 °C for 120 h. After the addition of 10 mM ethylene glycol and incubating for 15 min, the pH value was adjusted to 8 with 1 M NaOH and 20 mg sodium borohydride were added. Then, the soln was incubated at 20 °C for 18 h and finally neutralized with 0.5 M acetic acid. After concentration in a rotary evaporator at 30 °C, MeOH was added, and the drying procedure

was twice repeated. For dissolving the residue, 5 mM ammonium acetate was added (800 μL) and the soln containing the modified SCWP was subjected to GPC, which was performed as described above to furnish polysaccharide **3**. Lyophilized samples were dissolved in 5 mL of 1% acetic acid and incubated at 110 °C for 90 min under N_2. After cooling down to 20 °C, the soln was neutralized with dilute aq NH_3 and the samples were subjected to GPC. Appropriate fractions containing degraded SCWP were pooled, dialyzed against water (HPLC-grade), and lyophilized to afford polysaccharide **4**. In a separate approach, periodate-oxidation was performed on purified SCWP **1**, followed by $NaBH_4$ reduction and hydrolysis with 1% acetic acid at 110 °C for 1 h. Purification of the resulting material was performed on Superdex 75 with 0.05 M NH_4OAc as eluant followed by RP-HPLC on Nucleosil C_{18} with a gradient of aq MeCN containing 0.1% TFA. Separation of the oligomers from the polymeric fraction by RP-HPLC furnished a mixture of smaller fragments from which a fraction with trisaccharide **5** (1.5 mg) was isolated and investigated by MS and NMR-spectroscopy.

3.6. NMR-spectroscopy

All NMR spectra were recorded at 20 °C on a Bruker Avance 800 instrument at 799.96 MHz for proton and 201.12 MHz for carbon using a 5 mm cryo probe. The sample contained freeze-dried material dissolved in 120 μL D_2O in a 3 mm NMR tube or 600 μL D_2O in a 5 mm NMR tube. The ppm scales were calibrated to acetone for proton (2.22 ppm) and carbon (30.89 ppm), giving a HDO signal at 4.82 ppm. The NMR spectra were recorded using Bruker standard homo-nuclear pulse programs as cosydfphpr for DQF-COSY, noesyphpr for NOESY (100 ms mixing time), and mlevphpr for TOCSY (80 ms spinlock time). For hetero-nuclear experiments, apart from H2BC, Bruker standard pulse programs were used as hsqcedetgp, for one-bond proton–carbon correlated gHSQC, and hmbcgpl2ndqf for multiple bond correlated HMBC with suppression of one-bond correlations. Further information for the assignments was obtained by HSQC-TOCSY and HSQC-NOESY experiments using Bruker standard pulse programs hsqcetgpml and hsqcetgpnosp. In addition, H2BC spectra were recorded as described.[24] All homo-nuclear spectra were recorded with acquisition time of 0.3 s, 4k × 1k data points, and zero filled in both dimensions. All hetero-nuclear spectra were recorded with acquisition time of 0.12 s, 2k × 512 data points, and zero filled in both dimensions.

3.7. Mass-spectrometry

Samples were dissolved in the appropriate volume of water to give a soln of approx. 1 nmol/μL. For the analysis, an aliquot of the soln was diluted with 50% aq MeCN containing 0.1% formic acid to give a final concentration of ~10 pmol/mL. The soln was subjected to offline ESI-QTOFMS on a waters Micromass Q-TOF Ultima Global. Capillary voltage was adjusted to obtain approx. 200 counts/s. The MS instrument was tuned with [Glu1]-fibrinopeptide B to give the highest possible sensitivity and a resolution of ca. 10.000 (FWHM). Mass tuning of the analyzer was done in the tandem MS mode using [Glu1]-fibrinopeptide B. Data analysis was performed with MASSLYNX 4.0 SP4 Software (Waters Micromass). Additional matrix-assisted laser desorption/ionization time-of-flight (MALDI-TOF) measurements were performed on a Voyager-DE STR BioSpectrometry Workstation MALDI-TOF mass spectrometer (Perseptive Biosystems, Framingham, USA). Samples were prepared with a 2,5-dihydroxybenzoic acid (DHB) matrix consisting of 10 mg of the matrix dissolved in 1 mL of 0.3% trifluoroacetic acid in acetonitrile–water (1:1, v/v) and measured in the linear mode at an acceleration voltage of 25 kV. Each spectrum obtained was the mean of 256 laser shots.

Acknowledgments

The authors thank Dr. Daniel Kolarich for providing ESI-QTOF mass spectra. The spectra at 800 MHz were obtained on the Bruker Avance 800 spectrometer of the Danish Instrument Center for NMR Spectroscopy of Biological Macromolecules.

References

1. Sára, M.; Sleytr, U. B. *J. Bacteriol.* **2000**, *182*, 859–868.
2. Sleytr, U. B.; Messner, P.; Pum, P.; Sára, M. *Angew. Chem., Int. Ed.* **1999**, *38*, 1034–1054.
3. Sleytr, U. B.; Sára, M.; Pum, D.; Schuster, B. In *Supramolecular Polymers*; Ciferri, A., Ed.; CRC Press, Taylor & Francis Group: Boca Raton, USA, 2005; pp 583–616.
4. Birechtel, E.; Bahl, H. *J. Bacteriol.* **1999**, *181*, 5017–5023.
5. Cava, F.; de Pedro, M. A.; Schwarz, H.; Henne, A.; Berenguer, J. *Mol. Microbiol.* **2004**, *52*, 677–690.
6. Chauvaux, S.; Matuschek, M.; Beguin, P. *J. Bacteriol.* **1999**, *181*, 2455–2458.
7. Egelseer, E. M.; Leitner, K.; Jarosch, M.; Hotzy, C.; Zayni, S.; Sleytr, U. B.; Sára, M. *J. Bacteriol.* **1998**, *180*, 1488–1495.
8. Egelseer, E. M.; Danhorn, T.; Pleschberger, M.; Hotzy, C.; Sleytr, U. B.; Sára, M. *Arch. Microbiol.* **2001**, *177*, 70–80.
9. Huber, C.; Ilk, N.; Rünzler, D.; Egelseer, E. A.; Weigert, S.; Sleytr, U. B.; Sára, M. *Mol. Microbiol.* **2005**, *55*, 197–205.
10. Ilk, N.; Kosma, P.; Puchberger, M.; Egelseer, E. M.; Mayer, H. F.; Sleytr, U. B.; Sára, M. *J. Bacteriol.* **1999**, *181*, 7643–7646.

11. Ilk, N.; Völlenkle, C.; Egelseer, E. M.; Breitwieser, A.; Sleytr, U. B.; Sára, M. *Appl. Environ. Microbiol.* **2002**, *68*, 3251–3260.
12. Jarosch, M.; Egelseer, E. M.; Mattanovich, D.; Sleytr, U. B.; Sára, M. *Microbiology* **2000**, *146*, 273–281.
13. Jarosch, M.; Egelseer, E. M.; Huber, C.; Moll, D.; Mattanovich, D.; Sleytr, U. B.; Sára, M. *Microbiology* **2001**, *147*, 1352–1363.
14. Lemaire, M.; Miras, I.; Gounon, P.; Beguin, P. *Microbiology* **1998**, *144*, 211–217.
15. Mader, C.; Huber, C.; Moll, D.; Sleytr, U. B.; Sára, M. *J. Bacteriol.* **2004**, *186*, 1758–1768.
16. Mesnage, S.; Weber-Levy, M.; Haustant, M.; Mock, M.; Fouet, A. *Infect. Immun.* **1999**, *67*, 4847–4850.
17. Mesnage, S.; Fontaine, T.; Mignot, T.; Delepierre, M.; Mock, M.; Fouet, A. *EMBO J.* **2000**, *19*, 4473–4484.
18. Ries, W.; Hotzy, C.; Schocher, I.; Sleytr, U. B.; Sára, M. *J. Bacteriol.* **1997**, *179*, 3892–3898.
19. Rünzler, D.; Huber, C.; Moll, D.; Köhler, G.; Sára, M. *J. Biol. Chem.* **2004**, *279*, 5207–5215.
20. Sára, M. *Trends Microbiol.* **2001**, *9*, 47–49.
21. Engelhardt, H.; Peters, J. *J. Struct. Biol.* **1998**, *124*, 276–302.
22. Schäffer, C.; Müller, N.; Mandal, P. K.; Christian, R.; Zayni, S.; Messner, P. *Glycoconjugate J.* **2000**, *17*, 681–690.
23. Sára, M.; Dekitsch, C.; Mayer, H. F.; Egelseer, E. M.; Sleytr, U. B. *J. Bacteriol.* **1998**, *180*, 4146–4153.
24. Petersen, B. O.; Vinogradov, Y.; Kay, W.; Würtz, P.; Nyberg, N. T.; Duus, J. Ø.; Sørensen, O. W. *Carbohydr. Res.* **2006**, *341*, 550–556.
25. Garegg, P. J.; Jansson, P.-E.; Lindberg, B.; Lindh, F.; Lönngren, J.; Kvarnström, I.; Nimmich, W. *Carbohydr. Res.* **1980**, *78*, 127–132.
26. Leone, S.; Izzo, V.; Silipo, A.; Sturiale, L.; Garozzo, D.; Lanzetta, R.; Parrilli, M.; Molinaro, A.; Di Donato, A. *Eur. J. Biochem.* **2004**, *271*, 2691–2704.
27. Perlin, A. S. *Adv. Carbohydr. Chem. Biochem.* **2006**, *60*, 183–250.
28. Schäffer, C.; Messner, P. *Microbiology* **2005**, *151*, 643–651.
29. Bock, K.; Pedersen, C. *J. Chem. Soc., Perkin Trans. 2* **1974**, 293–297.
30. Schäffer, C.; Kählig, H.; Christian, R.; Schulz, G.; Zayni, S.; Messner, P. *Microbiology* **1999**, *145*, 1575–1583.
31. Steindl, C.; Schäffer, C.; Wugeditsch, T.; Graninger, M.; Mastecko, I.; Müller, N.; Messner, P. *Biochem. J.* **2002**, *368*, 483–494.
32. Steindl, C.; Schäffer, C.; Smrecki, V.; Messner, P.; Müller, N. *Carbohydr. Res.* **2005**, *340*, 2290–2296.
33. Choudhury, B.; Leoff, C.; Saile, E.; Wilkins, P.; Quinn, C. P.; Kannenberg, E. L.; Carlson, R. W. *J. Biol. Chem.* **2006**, *281*, 27932–27941.